

A contraction theory approach to observer-based controller design for glucose regulation in type 1 diabetes with intra-patient variability

Bhabani Shankar Dey^a, Anirudh Nath^{b,*}, Abhilash Patel^c, Indra Narayan Kar^a

^aDepartment of Electrical Engineering, Indian Institute of Technology Delhi, Hauz Khas, New Delhi, 110016, India

^bGE Global Research, Bengaluru, Karnataka, 560066, India

^cDepartment of Electrical Engineering, Indian Institute of Technology Kanpur, Kalyanpur, Kanpur, Uttar Pradesh, 208016, India

Abstract

While the Artificial Pancreas is effective in regulating the blood glucose in the safe range of 70-180 mg/dl in type 1 diabetic patients, the high intra-patient variability, as well as exogenous meal disturbances, poses a serious challenge. The existing control algorithms thus require additional safety algorithms and feed-forward actions. Moreover, the unavailability of insulin sensors in Artificial Pancreas makes this task more difficult. In the present work, a subcutaneous model of type 1 diabetes (T1D) is considered for observer-based controller design in the framework of contraction analysis. A variety of realistic multiple-meal scenarios for three virtual T1D patients have been investigated with $\pm 30\%$ of parametric variability. The average time spent by the three T1D patients is found to be 77%, 73% and 76%, respectively. A significant reduction in the time spent in hyperglycemia (> 180 mg/dl) is achieved without any feed-forward action for meal compensation.

Keywords: Artificial pancreas, observer, contraction analysis, intra-patient variability, nonlinear control

1. Introduction

Deficiency of insulin is prominent in type 1 diabetes patients (T1DPs) due to auto-immune destruction of the insulin-secreting β -cells in the pancreas. It results in prolonged elevated glucose levels (> 180 mg/dl) in the blood plasma, termed as hyperglycemia [1]. Thus the T1DPs have to rely upon insulin therapy in terms of multiple daily insulin injections to maintain normalcy in glucose level (70-180 mg/dl). In insulin therapy, dosage of insulin is manually calibrated for which requires the carbohydrate counting apriori [2]. Any overestimation or underestimation of carbohydrate counting can lead to inappropriate insulin dosages resulting in hyperglycemic (> 180 mg/dl) and hypoglycemic (< 70 mg/dl) episodes. Hyperglycemic and hypoglycemic instances can lead to ineffective glucose management in T1DPs. A large number of health-related complications, both macrovascular and microvascular, occur in T1DPs due to hyperglycemia and hypoglycemia [3, 4].

The issues as mentioned above can be addressed by the Artificial Pancreas (AP). The AP is an externally worn device equipped with a continuous micro-fluid insulin delivery system (insulin pump) and a glucose sensor. The performance of the AP is largely affected by (i) the delay in absorption of the subcutaneous insulin infusion [5], (ii) the circadian oscillations in insulin sensitivity [6] and (iii) the uncertainty in meal absorption [7]. Due to these factors, the T1DPs using AP face the

problem of postprandial hyperglycemia and late hypoglycemia [8]. The postprandial hyperglycemia refers to the sudden increase in glucose concentration after the meal intake. The late hypoglycemia refers to the sudden decrease in glucose concentration due to excessive insulin infusion at the time of the meal. So the existing APs often rely on additional feed-forward strategy and safety algorithms to achieve effective glucose regulation (70-180 mg/dl). The feedforward strategy requires accurate information about the carbohydrate contents of the meals to determine the insulin dosage required to compensate for the effect of the meal [9]. On the other hand, safety algorithms prevent excessive insulin infusion by estimating the existing insulin concentration in the body [10]. Thus, the focus of the current work hovers around achieving a tight glycemic control while minimizing the time spent in postprandial hyperglycemia and avoiding late hypoglycemia. In the current work, a model-based feedback control strategy is proposed that does not require any additional feedforward or safety algorithms.

The functionality of an automated AP can be divided into two steps: (i) the task of state estimation and (ii) the task of control design. The existing state estimation techniques and control algorithms for the AP is discussed current and succeeding paragraphs, respectively. A summary of a wide variety of state estimation techniques has been reported in the literature [5]. The main limiting factors of the success of the existing works on state estimation are intra-patient variability (variation of system parameters that occur inherently in the system) and uncertainty in the meal absorption dynamics [11]. There are several attempts to address these issues as in [11, 12, 13]. Still, this remains an open problem. The nature of the variability is unknown and, hence, poses some limitations to the current

*Corresponding Author: Anirudh Nath

Email addresses: bhabanishankar440@gmail.com (Bhabani Shankar Dey), anirudh.nath88@gmail.com (Anirudh Nath), apatel@iitk.ac.in (Abhilash Patel), ink@ee.iitd.ac.in (Indra Narayan Kar)

observers where specific assumptions on the uncertainty are involved. The Luenberger observer designs in [14, 15] are based on the nominal system and involve some linear approximations in the design. It can be too restrictive in terms of their applicability. A few robust nonlinear extended Luenberger observers have been designed in some recent studies [11, 12, 13] for addressing intra-patient variability. But there are some restrictive assumptions on the nature of uncertainty that may be difficult to be characterized in practice. On the other hand, the stochastic filtering approaches motivated by Kalman filtering (KF) techniques and its variants are quite common [16]. Algorithms like KFs [17], extended KFs [18] and unscented KFs [19, 20] have been proposed for state estimation in the AP problem. The requirement of precise information about the model, complex matrix computations, and the difficulty in the characterization of the probability distribution functions one to rethink before implementing them both in theory and practice while keeping in mind the unknown nature of parametric variability in T1DPs. An observer of extended Luenberger structure is proposed in the present work. The issues related to intra-patient variability and uncertainty in meal disturbance are addressed in the framework of contraction analysis [21].

The existing control algorithms for the AP is discussed from time to time in terms of several survey papers [22, 23, 24]. The main objectives of the current work are (i) to minimize the instances of postprandial hyperglycemia, and (ii) to avoid late hypoglycemic instances, in the presence of intra-patient variability. Mainly, two variants of robust controllers, namely the H_∞ control [25, 26, 27] and the sliding mode control (SMC) [28, 29] exist in the literature. The necessity of structural characterization of the bounded uncertainty and computational complexity makes the practical implementation of the H_∞ filter based controllers challenging. The chattering issues that are inevitable in SMC may trigger hypoglycemia during large intra-patient variability due to excessive insulin infusion [30]. Apart from these, most of the control algorithms are augmented with additional safety layers [23, 31, 32, 33] and meal compensation techniques (feed-forward action) [9]. It complicates the practical applications of such a multi-layered control approach [34]. Thus, an attempt is made in this current work to devise a simple feedback control law based on the theory of contraction analysis, which would be sufficient in itself to tackle these issues.

Contraction analysis offers an alternative tool for stability analysis of nonlinear systems, which has got lots of attraction recently [35]. The inherent feature of forgetting initial conditions exponentially makes it intriguing among control engineers to apply its principle in this problem [36]. Contraction theory is used in applications like observer design in [37, 38]. As compared to the stability analysis of uncertain nonlinear systems in the framework of Lyapunov stability, contraction analysis offers a more relaxed framework for the same. For instance, high uncertainty and time variability in the physiological parameters like insulin sensitivity, parameters related to insulin absorption and meal absorption, etc. that exist in T1DPs. As a result, there exists a complicated shifting of the equilibrium concerning the variability in system parameters. This may complicate the Lyapunov stability analysis, and getting a closed-form expression

of equilibria in respect of parameters may not be possible [39]. This problem can be circumvented by using contraction analysis.

In the present work, a nonlinear observer-based design of the control algorithm is proposed for the APS that considers the IVP model in [40]. The main highlights of the proposed state estimation based control technique is provided as follows:

- (i) A nonlinear observer is designed for estimating the glucose and insulin concentrations based on the contraction theory approach. The unknown observer gains are computed by solving a set of linear inequalities.
- (ii) The information about the estimated state variables are exploited to design a feedback control law for the glucose regulation under variability in insulin sensitivity and uncertainty in insulin absorption in the subcutaneous compartment.
- (iii) In comparison to the works in [41, 42], the proposed control algorithm involves the estimation of insulin concentration in the presence of uncertainty in parameters. Hence it is not required to augment any additional safety layers [31] like insulin-on-board (IOB) [10] to avoid post-prandial hyperglycemia [41]. It also avoids any type of additional feed-forward compensating action for disturbance rejection [9].
- (iv) The proposed strategy allows us to design the observer and the controller separately. The overall closed loop system, including controller and observer together, is shown to be stable using the concept of partial contraction theory.

The remaining part of this work is presented in several sections as follows. Section 2 presents the methodology of the current work. It further consists of four subsections that present the mathematical model, theoretical background, observer design, and controller design. Section 3 contains the closed-loop studies' results to show the effectiveness of the theoretical results. In Section 4, the summary of the work is briefly provided.

2. Methods

In this section, the dynamical model of the glucoregulatory system of T1DP is presented in the first subsection. In the second subsection, a brief background on contraction analysis is included. The third and fourth subsections, the details about the observer and controller design methodologies are provided.

2.1. Mathematical model

A model plays an important role in the effectiveness of the closed-loop control strategy. A large number of mathematical models are available in the existing literature that models the dynamics of the glucose-insulin interactions in T1DPs with varying levels of abstractions and utility, as mentioned in [43]. The complexity of these models, in terms of a large number of state variables and complicated nonlinear functions, limit their relevance to control applications [44]. Recently, a few variants of control-oriented subcutaneous models of T1DPs have been reported in the literature [45, 46, 47, 40]. The model in [40] is

adopted here due to its structural simplicity and identifiability. It is very important, especially in the context of personalising a control technique for individual patients.

2.1.1. State space representation

The Medtronic Virtual Patient (MVP) [46] models the glucose-insulin dynamics of type 1 diabetes in terms of a coupled ordinary differential equations (ODE) as

$$\begin{aligned}\dot{x}_1 &= -p_1x_1 - x_1x_2 + EGP + R_a(t) \\ \dot{x}_2 &= -p_2x_2 + p_3x_3 \\ \dot{x}_3 &= -p_4x_3 + p_4x_4 \\ \dot{x}_4 &= -p_5x_4 + p_6u(t)\end{aligned}\quad (1)$$

where the state vector $x = [x_1 \ x_2 \ x_3 \ x_4]^T$ represents the blood glucose concentration (mg/dl), the effective insulin in the blood (min^{-1}), the plasma insulin concentration (mU/l) and the subcutaneous insulin concentration (mU/l), respectively. The physiological parameter, p_1 denotes the glucose effectiveness, $\frac{p_2}{p_1}$ represents the insulin sensitivity factor, p_4 represents the time constant of the plasma insulin, p_5 denotes the time constant of the subcutaneous insulin and EGP stands for the endogenous glucose production. The values of the parameters are adopted from [46] as provided in Table 1. The blood glucose concentration is the output, y of the system (1), as mentioned below.

$$y = Cx = x_1 \quad (2)$$

where $C = [1 \ 0 \ 0 \ 0]$ is the output matrix.

The equilibrium state of the system in (1) is given as, $[x_1 \ x_2 \ x_3 \ x_4]^T = [EGP/p_1 \ 0 \ 0 \ 0]^T$. To shift this non-zero equilibrium to the origin, a translation operation is performed in the original state space. Thus, the resulting deviated state can be expressed as

$$[x_{1d} \ x_{2d} \ x_{3d} \ x_{4d}]^T = [x_1 \ x_2 \ x_3 \ x_4]^T - [EGP/p_1 \ 0 \ 0 \ 0]^T \quad (3)$$

where $(\cdot)^T$ represents the transpose operator. The corresponding deviated dynamics of the system (1) can be obtained as

$$\begin{aligned}\dot{x}_{1d} &= -p_1x_{1d} - \frac{EGP}{p_1}x_{2d} - x_{1d}x_{2d} + R_a(t) \\ \dot{x}_{2d} &= -p_2x_{2d} + p_3x_{3d} \\ \dot{x}_{3d} &= -p_4x_{3d} + p_4x_{4d} \\ \dot{x}_{4d} &= -p_5x_{4d} + p_6u(t).\end{aligned}\quad (4)$$

The corresponding output equation is expressed as

$$y = Cx = x_{1d} \quad (5)$$

2.1.2. Meal disturbance model

The meal disturbance model represents the dynamics of the glucose absorption in the gut and its appearance in the blood circulation following the meal intake. As mentioned in [48], the dynamics can be modelled as a two-compartmental model, as provided below

$$\begin{aligned}\dot{d}_1 &= -\frac{d_1}{t_{max}} + Bio \times Carb(t) \\ \dot{d}_2 &= \frac{d_1}{t_{max}} - \frac{d_2}{t_{max}} \\ R_a(t) &= \frac{d_2}{t_{max}}\end{aligned}\quad (6)$$

where d_1 and d_2 are the amount of glucose in the first and second compartments (mg/dl), t_{max} denotes the time-to-maximum rate of appearance of glucose in the blood (min), t is the time of meal intake (min), $Carb(t)$ denotes the ingested amount of carbohydrates at time t (mg/dl/min), Bio is carbohydrate bioavailability of the meal (unitless) and $R_a(t)$ represents glucose absorption rate (mg/dl/min) in the gut. The values of the parameters are adopted from [48] as $t_{max} = 43$ min and $Bio = 71$.

2.2. Preliminaries on Contraction Theory

Contraction theory helps to characterise the temporal behaviour of trajectories for a dynamical system to each other [49]. The system is said to be contracting if two arbitrary trajectories converge towards each other, forgetting their initial conditions. Fig. 1 depicts a pictorial representation of two arbitrary trajectories converging towards each other. The use of contraction theory relaxes the prior knowledge of equilibrium and ensures inherent robustness to disturbance. Here, we briefly present results from contraction theory, which will be used in subsequent sections.

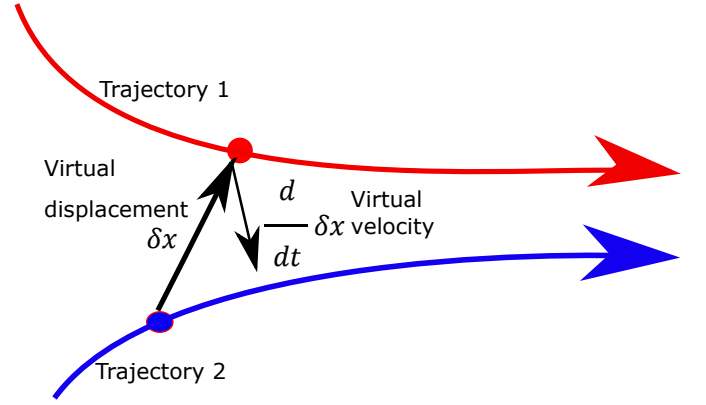


Figure 1: Two trajectories contracting to each other in a contracting region.

Consider a nonlinear dynamical system,

$$\dot{x} = f(x), \quad (7)$$

where $x \in \mathbf{R}^n$ is the system states, $f(x)$ is the drift function $f : \mathbf{R}^n \rightarrow \mathbf{R}^n$. The differential dynamics of the system (7) is,

$$\delta\dot{x} = \frac{\partial f}{\partial x} \delta x = J(x)\delta x, \quad (8)$$

where δx is the virtual displacement of infinitesimal perturbation in x , $J(x)$ is the Jacobian matrix of $f(x)$. The evolution of virtual displacement can be inferred using (8) as,

$$\frac{d}{dt}(\delta x^T \delta x) = 2\delta x^T \frac{\partial f}{\partial x} \delta x \leq 2\lambda_{max}(J)\delta x^T \delta x \quad (9)$$

where $\lambda_{max}(J)$ is the largest eigenvalue of the Jacobian J . If $\lambda_{max}(J)$ is strictly uniformly negative, then any infinitesimal length $|\delta x|$ converges exponentially to zero. Hence, all system trajectories of (7) will converge towards each other, forgetting their initial conditions, as illustrated in Fig. 1. If $\lambda_{max}(J)$ is negative in a set, such is called an invariant set, and the region

Table 1: Estimated parameters for different subjects [40].

Subjects	p_1	p_2	p_3	p_4	p_5	EGP	p_6
1	2.20×10^{-3}	1.06×10^{-2}	8.60×10^{-6}	0.0213	0.0204	1.33	1.02×10^{-5}
3	3.50×10^{-3}	2.33×10^{-2}	1.079×10^{-5}	0.0143	0.0141	1.07	1.55×10^{-5}
5	4.33×10^{-3}	9.63×10^{-3}	1.974×10^{-6}	0.0217	0.0217	0.6	1.416×10^{-5}

is called a contraction region. In this research article to prove this negative definiteness, we have used the contraction analysis based on matrix measure, which is alternatively known as logarithmic norm. Matrix measure, often referred to as $\mu(J)$ is defined as the directional derivative associated with the induced matrix norm evaluated at identity matrix in the direction of matrix (J) [50]. It should be noted that, if the vector norm is the standard Euclidean norm, then induced matrix measure is the largest eigenvalue of the symmetric part of (J) . Based on the different vector norms, different matrix measures can be referred to from Table 2.

Table 2: Matrix measure of real matrix $A = [a_{ij}]$ corresponding to different vector norms [51].

Vector Norms $\ (\cdot)\ $	Corresponding Matrix Measure, $\mu(A)$
$\ x\ _1 = \sum_{i=1}^n x_i $	$\mu_1(A) = \max_j (a_{jj} + \sum_{i \neq j} a_{ij})$
$\ x\ _2 = (\sum_{i=1}^n x_i ^2)^{\frac{1}{2}}$	$\mu_2(A) = \lambda_{\max}(\frac{A+A^T}{2})$
$\ x\ _\infty = \max_{1 \leq i \leq n} x_i $	$\mu_\infty(A) = \max_i (a_{ii} + \sum_{i \neq j} a_{ij})$

Definition 2.1. Uniform negative definiteness of Jacobian $J(x)$ means there exist a positive constant β such that $(J(x)^T + J(x)) < -\beta I < 0$ in a region $\Omega \subset \mathbf{R}^n$ for $\forall t > 0$.

A relaxed form as partial contraction analysis extends contraction analysis for convergence to a specific behavior. It has been applied to the synchronization of oscillators [36] and observer design [52].

Lemma 1. Consider a nonlinear system of the form

$$\dot{x} = f(x, x)$$

and assume that the auxiliary system (a.k.a virtual system)

$$\dot{y} = f(y, x)$$

is contracting to y . If a particular solution of the auxiliary y -system verifies a smooth the specific property, then all trajectories of the original x -system verify this property exponentially. The original system is said to be partially contracting.

The proof of this lemma is presented in [53]. If the virtual system admits two particular solutions and contracting in nature, then two particular solutions will converge towards each other. The design understanding should be to design a virtual system that will have estimator dynamics as a particular solution and system dynamics as another particular solution. The salient property of contraction analysis is that it can quantify the robustness of an external perturbation.

Lemma 2. Consider that the nominal system

$$\dot{x} = f(x)$$

is contracting and the perturbed model

$$\dot{x}_p = f(x_p) + d(t),$$

where x_p is the perturbed state, $d(t)$ be a vanishing perturbation satisfying $|d(t)| \leq c_1 e^{-c_2 t}$ for some $c_1, c_2 > 0$ and $t \geq 0$. Then, there exist constants $k_1, k_2 > 0$ such that the following property holds $\forall t > 0$

$$|x(t) - x_p(t)| < e^{-k_1 t} (k_2 + |x_0 - z_0|) \quad (10)$$

2.3. Observer Design for Artificial Pancreas

As discussed in Section 1, the state estimation algorithm is necessary to retrieve information about insulin concentrations in the body, which is of paramount importance in the case of a practical APS. A nonlinear observer of the extended Luenberger structure is considered for estimating the state variables concerning glucose and insulin concentrations in the plasma and subcutaneous compartments. The dynamical equations of the observer for the system in (1) are provided below

$$\begin{aligned} \dot{\hat{x}}_1 &= -p_1 \hat{x}_1 - \hat{x}_2 x_1 + EGP + l_1 (\hat{x}_1 - x_1) \\ \dot{\hat{x}}_2 &= -p_2 \hat{x}_2 + p_3 \hat{x}_3 + l_2 (\hat{x}_1 - x_1) \\ \dot{\hat{x}}_3 &= -p_4 \hat{x}_3 + p_4 \hat{x}_4 + l_3 (\hat{x}_1 - x_1) \\ \dot{\hat{x}}_4 &= -p_5 \hat{x}_4 + u(t) + l_4 (\hat{x}_1 - x_1) \end{aligned} \quad (11)$$

where $\hat{x}_i, i = 1, \dots, 4$ are the estimated system states and $L = [l_1 \ l_2 \ l_3 \ l_4]^T$ is the unknown observer gain needs to be selected to ensure the convergence of estimated state, $\hat{x}_i, i = 1, \dots, 4$ in (11) to the true states, $x_i, i = 1, \dots, 4$ in (1). The existence and computation of the observer gain, L is stated in the form of following theorem.

Theorem 1. Consider the system dynamics in (1) and the observer in (11) with the observer gain, $L = [l_1 \ l_2 \ l_3 \ l_4]$. The estimated states, \hat{x}_i in (11) will converge to the true states, x_i in (1), exponentially from arbitrary initial conditions if the observer gain L satisfies the following linear inequalities

$$\begin{aligned} -p_1 + l_1 + l_2 + l_3 + l_4 &< 0 & -p_2 + x_1 &< 0 \\ -p_4 + p_3 &< 0 & -p_5 + p_4 &< 0. \end{aligned} \quad (12)$$

Proof. Let us consider a virtual system as

$$\begin{aligned} \dot{s}_1 &= -p_1 s_1 - x_1 s_2 + EGP + l_1 (s_1 - x_1) \\ \dot{s}_2 &= -p_2 s_2 + p_3 s_3 + l_2 (s_1 - x_1) \\ \dot{s}_3 &= -p_4 s_3 + p_4 s_4 + l_3 (s_1 - x_1) \\ \dot{s}_4 &= -p_5 s_4 + u(t) + l_4 (s_1 - x_1) \end{aligned} \quad (13)$$

where $s_i, i = 1, \dots, 4$ are the states of virtual system. It has two particular solutions. For $s_i = x_i$, the virtual system represents the system dynamics in (1), and for $s_i = \hat{x}_i$, the virtual system represents the observer dynamics in (11). Now, the corresponding differential dynamics of the virtual system in (13) can be obtained as

$$\begin{bmatrix} \delta \dot{s}_1 \\ \delta \dot{s}_2 \\ \delta \dot{s}_3 \\ \delta \dot{s}_4 \end{bmatrix} = \begin{bmatrix} -p_1 + l_1 & -x_1 & 0 & 0 \\ l_2 & -p_2 & p_3 & 0 \\ l_3 & 0 & -p_4 & p_4 \\ l_4 & 0 & 0 & -p_5 \end{bmatrix} \begin{bmatrix} \delta s_1 \\ \delta s_2 \\ \delta s_3 \\ \delta s_4 \end{bmatrix} \quad (14)$$

In the compact form, the differential dynamics becomes

$$\delta \dot{s} = J \delta s \quad (15)$$

If the matrix measure of J , in (15) is negative, then the virtual system dynamics in (13) will be contracting. So, one needs to choose the observer gains, $L = [l_1 \ l_2 \ l_3 \ l_4]^T$ in such a way that $\mu_1(\cdot) < 0$. (Here, the matrix measure is based on 1-norm). Referring to Table 2, the conditions for the observer gains can be computed as in (12). If the inequalities in (12) are satisfied, then the virtual system in (13) will be a contracting system. Hence, by Lemma 1, it can be inferred that the estimated states, \hat{x}_i in (11) converges to the corresponding true states, x_i in (1) exponentially. \square

From the physiological knowledge, it is well known that state x_1 (blood glucose concentration) evolve in a compact set X [22]. Thus, the compact set's boundary values can be substituted as an argument to the inequality in (12) and tune the observer gain to satisfy the inequality.

Remark 1. It is important to note that the inequalities in (12) involve only the information of blood glucose concentration, x_1 , which is the measurable quantity in AP. It provides less conservatism than the observer designs in [11, 12, 13]. This is because of the requirement of information on the bounds of all the state variables. Apart from blood glucose concentration, it is difficult to get the bounds of other state variables precisely.

Remark 2. The contraction theory provides us with an alternative approach for observer design in contrast to the Lyapunov stability theory. Furthermore, the observer designs in [11, 12, 13] are based on quadratic Lyapunov functions and involve linear approximations of the nonlinearity, such as Lipschitz condition [13] and one-sided quasi-Lipschitz condition. Unlike these methods, the proposed observer in (11) is less conservative since it does not require any of the above mentioned assumptions.

2.3.1. Estimation results:

The performance of the observer is evaluated in terms of estimation of the plasma glucose concentration and the plasma insulin concentration for three T1D subjects. A hypothetical 24 h scenario is considered with the assumption that the T1D subjects receive a single meal of 70 g carbohydrate at $t=10$ min

followed by a fasting period. The parameters of the T1D subjects are referred from Table 1. The initial conditions are chosen as $x_1=120$ mg/dl, $x_2 = 0.01 \text{ min}^{-1}$, $x_3 = 1$ mU/l and $x_4 = 1$ mU/l. Observer gains are chosen by satisfying the inequalities in (12) while considering minimum glucose concentration ($x_1 = 0$ mg/dl). The corresponding results of the state estimation are depicted in Fig. 2. It can be observed that the convergence of the estimate \hat{x}_1 to the true state x_1 is very fast for all the cases. Although \hat{x}_3 converges to the actual state x_3 in a finite time, the convergence in case of T1D Subject 1 is comparatively slower than Subjects 2 and 3. Here, it is verified that the observer is capable of estimating both the glucose and insulin concentrations. Next, the design of the control law based on the contraction analysis is presented.

2.4. Controller Design for Artificial Pancreas

The most important feature that an effective control law should possess for its implementation in APS is that it should avoid severe hypoglycemia ($x_1 < 50$ mg/dl) at any circumstance. Additionally, it should ensure an automated continuous insulin delivery to minimize the postprandial glucose excursions and minimize the risks of hyperglycemia ($x_1 > 180$ mg/dl). The blood glucose should be below 180 mg/dl within 1 h after meal intake. All these control objectives need to be achieved by utilizing the state estimates provided by the observer and in the presence of parametric uncertainty and exogenous meal disturbances.

The convergence of the estimated states to the actual states has been already established in Theorem 1. In the next step, the deviated dynamics in (4) is considered to formulate the control problem as a regulation problem. By ensuring the deviated state x_d converge to zero, the actual states converge to the equilibrium point. To achieve this objective, the a feedback proportional control law is chosen as

$$u = K \hat{x}_d \quad (16)$$

where $K = [k_1 \ k_2 \ k_3 \ k_4]$ is the controller gain matrix and $\hat{x}_d = [\hat{x}_{1d} \ \hat{x}_{2d} \ \hat{x}_{3d} \ \hat{x}_{4d}]^T$ is the estimate of the deviated state, $x_d = [x_{1d}, x_{2d}, x_{3d}, x_{4d}]^T$. The information of \hat{x}_d can be extracted from the transformation to the estimated states \hat{x} as introduced in (3) as

$$[\hat{x}_{1d} \ \hat{x}_{2d} \ \hat{x}_{3d} \ \hat{x}_{4d}]^T = [\hat{x}_1 \ \hat{x}_2 \ \hat{x}_3 \ \hat{x}_4]^T - [EGP/p_1 \ 0 \ 0 \ 0]^T. \quad (17)$$

The estimation error can be obtained as

$$e = x_d - \hat{x}_d \quad (18)$$

By substituting the control law in (16), the closed loop deviated dynamics (4) can be re-written in compact form as

$$\dot{x}_d = f(x_d) + BK \hat{x}_d \quad (19)$$

which can be re-written as

$$\begin{aligned} \dot{x}_d &= f(x_d) + BK(x_d - e) \\ &= f(x_d) + BKx_d - BKe \\ &= f(x_d)_{CL} + d(t) \end{aligned} \quad (20)$$

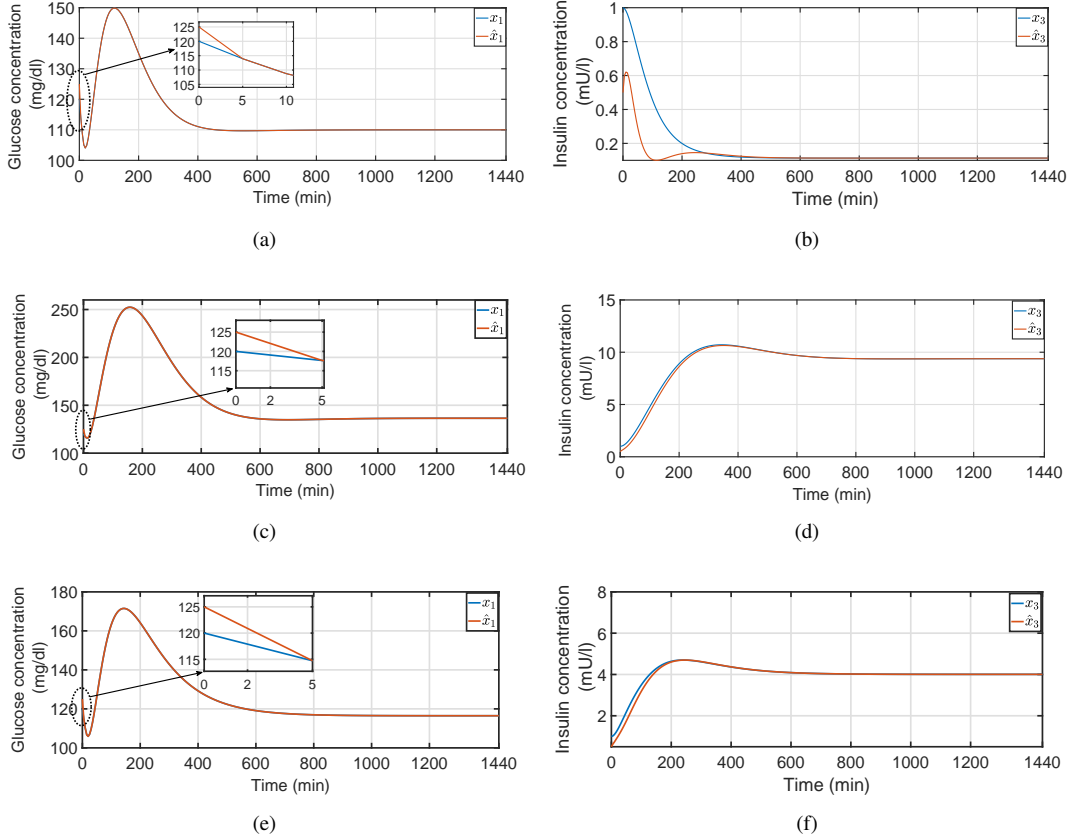


Figure 2: Results for the estimation of plasma glucose concentration and plasma insulin concentration of (a) subject 1, (b) subject 2 and (c) subject 3.

where $f(x_d)_{CL} = f(x_d) + BKx_d$ and $d(t) = -BKe$. In general, for a state-feedback based control law, $u = K\hat{x}_d$, the controller gain matrix, K needs to be designed. The controller gains, $k_i, i = 1, \dots, 4$ in (16) need to be selected to ensure the stability of closed loop system that includes the observer states in (11) and the control law in (16). The stability analysis of closed loop system using contraction theory is presented in the form of following theorem.

Theorem 2. Consider the closed loop system in (20) with $d(t) = -BKe(t)$ be the vector function satisfying $|d(t)| \leq c_1 e^{-c_2 t}$, there exist a controller gain matrix, $K = [k_1, k_2, k_3, k_4]^T$ dictated by the following relations in (21) such that $f(x_d)_{CL}$ is contracting.

$$\begin{aligned} -p_1 - x_{2d} + k_1 p_6 &< 0 \\ -p_2 + k_2 p_6 + (EGP/p_1) - x_{1d} &< 0 \\ -p_4 + p_3 + k_3 p_6 &< 0 \\ k_4 p_6 - p_5 + p_4 &< 0, \end{aligned} \quad (21)$$

The states of closed loop system (controller-observer put together) will exponentially converge to the equilibrium. Further, it will imply that the following relation will be satisfied

$$|x_d| < e^{-\alpha_1 t} (\alpha_2 t + |x_{d0}|) \quad (22)$$

where $\alpha_1, \alpha_2 > 0$ are two positive constants that depend upon the initial conditions and the minimum contraction rates of the observer and the system.

Proof. The proof of the above theorem is straightforward as stated below. Consider the closed loop dynamics as mentioned in (20)

$$\text{where } f(x_d) = \begin{bmatrix} -p_1 x_{1d} + (EGP/p_1)x_{2d} - x_{1d}x_{2d} \\ -p_2 x_{2d} + p_3 x_{3d} \\ -p_4 x_{3d} + p_4 x_{4d} \\ -p_5 x_{4d} \end{bmatrix}, B = \begin{bmatrix} 0 \\ 0 \\ 0 \\ p_6 \end{bmatrix}$$

then $f(x_d)_{CL}$ becomes

$$f(x_d)_{CL} = \begin{bmatrix} -p_1 x_{1d} + (EGP/p_1)x_{2d} - x_{1d}x_{2d} \\ -p_2 x_{2d} + p_3 x_{3d} \\ -p_4 x_{3d} + p_4 x_{4d} \\ -p_5 x_{4d} \end{bmatrix} + \begin{bmatrix} 0 \\ 0 \\ 0 \\ p_6 \end{bmatrix} \begin{bmatrix} k_1 \\ k_2 \\ k_3 \\ k_4 \end{bmatrix}^T \begin{bmatrix} x_{1d} \\ x_{2d} \\ x_{3d} \\ x_{4d} \end{bmatrix}$$

In compact form,

$$f(x_d)_{CL} = \begin{bmatrix} -p_1 x_{1d} + (EGP/p_1)x_{2d} - x_{1d}x_{2d} \\ -p_2 x_{2d} + p_3 x_{3d} \\ -p_4 x_{3d} + p_4 x_{4d} \\ -p_5 x_{4d} + p_6 k_1 x_{1d} + p_6 k_2 x_{2d} + p_6 k_3 x_{3d} + p_6 k_4 x_{4d} \end{bmatrix} \quad (23)$$

The differential dynamics of closed loop system is in the form,

$$\delta \dot{x}_d = J_c \delta x_d \quad (24)$$

$$\text{where } J_c = \begin{bmatrix} -p_1 - x_{2d} & (EGP/p_1) - x_{1d} & 0 & 0 \\ 0 & -p_2 & p_3 & 0 \\ 0 & 0 & -p_4 & p_4 \\ k_1 p_6 & k_2 p_6 & k_3 p_6 & k_4 p_6 - p_5 \end{bmatrix}$$

Similar to the observer design in 2.3, the controller gain K can be selected in the framework of partial contraction stated in Lemma 1. Therefore, designed K will ensure the closed loop system ($f(x_d)_{nominal}$) to be contracting to equilibrium and $e(t) \rightarrow 0$ exponentially as the observer dynamics achieves exponential convergence. Here, the term $d(t) = -BKe(t)$ can be treated as a decaying perturbation to the nominal system. Using Lemma 2, exponential convergence of states to the equilibrium is guaranteed as given in (22). \square

For the nominal system to be contracting, we need to design K such that the matrix measure of J_c is negative. Using matrix measure, the design conditions can be obtained as (21).

Remark 3. It is important to highlight that the observer and controller design can be carried out separately. The reason behind this is that the system comprising of the cascade interconnection of two individually contracting systems, is also contracting [35]. Hence, this work is less restrictive than the other works on observer-based controller in [11, 12, 13].

3. Results

For evaluating the efficacy of the proposed observer-based control technique, two broad simulation categories are undertaken as case studies. The first category represents a realistic daily scenario of T1D patients, where three meals of 75 g carbohydrates, a representative of breakfast, lunch, and dinner, are taken into consideration. The corresponding observer and controller gains are chosen based on the inequalities in (12) and (21), respectively.

3.1. Scenario 1: A single day, three meal scenario with nominal parameters

The T1D model, as presented in (1), is being considered to represent the T1DPs. This virtual simulation scenario of 24 h (equivalent to 1440 min) is designed to investigate the performance of the controller in addressing inter-patient variability. So three virtual T1DPs, namely, Subjects 1, 3, and 5, are taken into consideration and the corresponding parameters are adopted from [40] as mentioned in Table 1. Three meals containing an equal amount of carbohydrate of 75 g are provided as breakfast, lunch, and dinner at $t=10, 360,$ and 720 min, respectively. It is assumed that the simulations start from a safe blood glucose level, x_1 of 120 mg/dl and initial conditions $x_2 = 0.01 \text{ min}^{-1}$, $x_3 = 1 \text{ mU/l}$ and $x_4 = 1 \text{ mU/l}$.

As illustrated in Fig. 3, the glucose concentration is effectively regulated within the euglycemic range ($x_1 \in [70 - 180]$ mg/dl) for all the three T1D subjects taken under consideration. In the case of Subject 3, there is a glucose excursion above 180 mg/dl in the postprandial period after the first meal. However, the glucose is brought below the hyperglycemic clamp

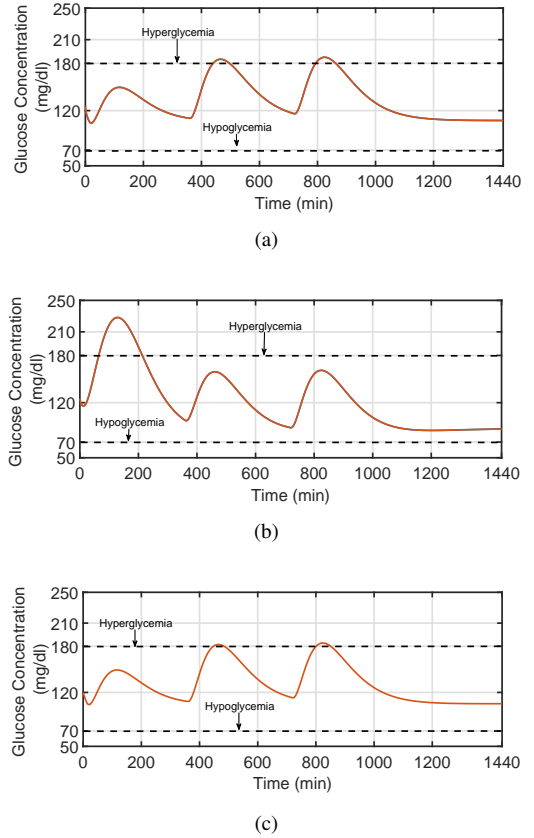


Figure 3: Plasma glucose concentration trajectories of (a) subject 1, (b) subject 2 and (c) subject 3 under the proposed observer-based feedback control law.

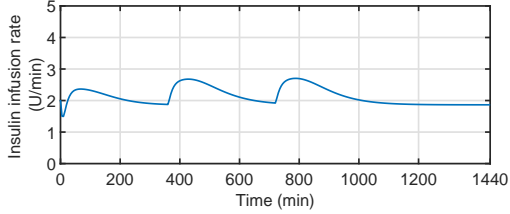
($x_1 = 180$ mg/dl) within two hours. During the whole simulation period, no instance of hypoglycemic ($X - 1 < 70$ mg/dl) episodes are recorded for all the cases. It validates the ability of the proposed control algorithm in the nominal conditions. The corresponding control signals in terms of the exogenous subcutaneous insulin infusion rate are shown in Fig. 4. It can be observed that an almost constant insulin delivery rate is maintained for the 24 h simulations. It is important to highlight that there is a transient increase in insulin delivery rate when there is a transient growth in glucose level after meal intakes. This feature of the control law is highly desirable for minimising the risks of postprandial hyperglycemia. The smooth profile of the exogenous insulin delivery rate makes the controller action less aggressive, which can help avoid late hypoglycemia induced by excessive insulin infusion if any.

3.2. Scenario 2: A single day, 3 meal scenario with intra-patient variability

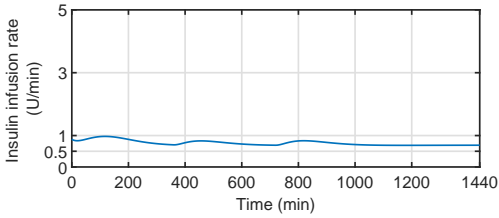
The main focus of the current scenario is to investigate the effect of bounded parametric uncertainty on the closed-loop performance. Four different simulation settings are further considered that take explicit variability in insulin sensitivity (IS), insulin pharmacokinetics and pharmacodynamics, and the initial conditions of glucose and insulin in the body. The observer and the controller feedback parameters are computed only for the T1D patients considering the nominal parameter values. For

Table 3: Simulation setting for Scenario 2A-2D for T1D Subjects 1, 3 and 5.

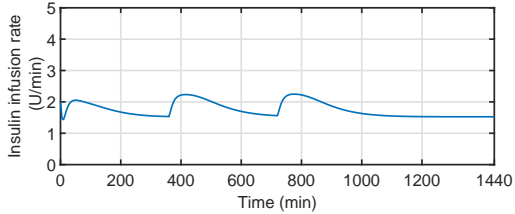
Scenario	Parameters					Initial conditions			
	p_1	p_2	p_3	p_4	p_5	x_{10}	x_{20}	x_{30}	x_{40}
2A	Nominal	Nominal	$\pm 30\%$	Nominal	Nominal	120	0.1	1	1
2B	Nominal	Nominal	Nominal	$\pm 30\%$	$\pm 30\%$	120	0.1	1	1
2C	$\pm 30\%$	120	0.1	1	1				
2D	$\pm 30\%$	[80 140]	0.01	[0 10]	1				



(a)



(b)



(c)

Figure 4: Insulin infusion rate as suggested by the proposed observer-based feedback control law for (a) subject 1, (b) subject 2 and (c) subject 3.

testing the robustness of the proposed technique, these feedback parameters are kept constant for each subject. One hundred numerical simulations are carried out for each of the T1D subjects with random parametric perturbations. The different protocols of this scenario are provided in Table 3. The details about the different simulation settings are presented below.

3.2.1. Scenario 2A: Variability in insulin sensitivity (IS)

IS can be critical physiological parameters responsible for variability in the glucose stabilization in T1DPs. The parameter, p_3 that is directly related the IS and is assumed to vary in a range of $\pm 30\%$ of its nominal value. A total of 100 simulations are carried out with randomly varying p_3 in $\pm 30\%$ uncertainty bound specified in Table 3.

From Table 4, it can be inferred that the proposed control law is highly efficient in dealing with the uncertainty in IS as noted in Table 3. For all the cases, percentage of time spent

in euglycemic range ($x_1 \in [70 - 180]$ mg/dl) is more than 84% and that in hyperglycemic range ($x_1 > 180$ mg/dl) is less than 16%. No hypoglycemia ($x_1 < 70$ mg/dl) or severe hypoglycemia ($x_1 < 50$ mg/dl) observed from the simulation results with variable IS.

Table 4: Percentage of time spent by the the virtual patients in the euglycemic ($x_1 \in [70 - 180]$ mg/dl), hyperglycemic ($x_1 > 180$ mg/dl) and hypoglycemic ($x_1 \in [50 - 70]$ mg/dl).

Subject	Scenario No.	Time Spent in euglycemic range (%)	Time spent in hyperglycemic range (%)	Time spent in hypoglycemic range (%)
Subject 1	2A	84.08	15.92	0
	2B	100	0	0
	2C	77.85	22.15	0
	2D	46.37	53.63	0
Subject 3	2A	87.20	12.80	0
	2B	69.55	30.45	0
	2C	78.89	21.11	0
	2D	59.86	40.14	0
Subject 5	2A	92.73	7.27	0
	2B	92.04	7.96	0
	2C	76.82	23.18	0
	2D	42.21	57.79	0

3.2.2. Scenario 2B: Variability in insulin pharmacokinetics and pharmacodynamics

The variation in the insulin absorption dynamics due to the uncertainty in the parameters, p_j , $j = 4, 5$, is also significant. A variation of $\pm 30\%$ about nominal values is assumed to carry out 100 numerical simulations for the T1D subjects. During each simulation, the parameters are randomly initialized from the uncertainty bound is given in Table 3.

From Table 4, it can be concluded that the designed controller possesses the right capability to handle the issues related to the uncertainty in the subcutaneous insulin absorption. The percentage of time spent in the euglycemic range is 84% and 100% for Subjects 1 and 5, respectively. While in the case of Subject 3, it is around 70%. The time spent in hypoglycemia ($x_1 < 70$ mg/dl) is 0% as provided in Table 4.

3.2.3. Scenario 2C: Variability in all model parameters

Next, an uncertain case is considered where all the system parameters, p_i , $i = 1, \dots, 5$, are varied in the range $\pm 30\%$. The

objective of this scenario is to determine the effectiveness of the proposed technique in ensuring an efficient glucose regulation.

In this case study, Subjects 1, 3, and 5 spent almost 76% of the total time in the euglycemic range. The corresponding time spent above 180 mg/dl is below 22% for all the cases. Still, it is a significant improvement of glycemic control under a wide range of variation in all the system parameters. Complete avoidance of hypoglycemic instances has been recorded in this case, as presented in Table 4.

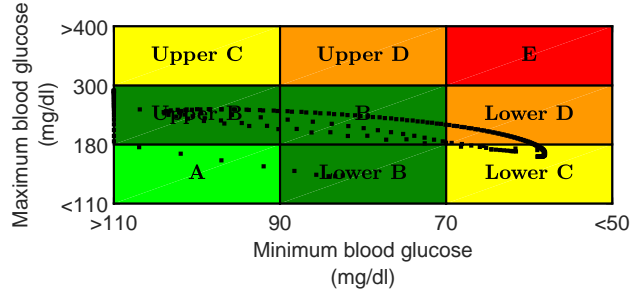


Figure 5: CVGA for parametric variability of $\pm 30\%$

3.2.4. Scenario 2D: Variability in initial values of glucose and insulin

To further complicate the situation, it is assumed that the initial glucose concentration varies within $x_1 \in [80 - 140]$, and the initial insulin concentration vary within $x_3 \in [0 - 10]$ mU/l. Like in the previous case, the parameters $p_i, i = 1, \dots, 5$ are assumed to vary in the range of $\pm 30\%$. The details of the protocol can be referred to from Table 3. A control variability grid analysis (CVGA) [15] is performed to evaluate the efficacy of the proposed observer-based control technique as illustrated in Fig. 5.

As depicted in Fig. 5, all the black dots are confined to Grid A, B, Upper B, Lower B, Lower D, and Lower C in the CVGA plot. There are a total of 300 dots (100 dots per subject with random parameters and initial conditions), which correspond to 300 random simulations in total. Each of these dots is mapped to a particular co-ordinate in the CVGA plot (depending upon the maximum and minimum glucose level achieved during the simulation). Severe hypoglycemia, i.e., glucose level below 50 mg/dl, is successfully avoided in all of these random numerical simulations. Approximately, 75% of the dots are confined to the safe grids (shown in green). Although 15% (approx) are in Grid Lower D and Grid Lower C, they are still above 50 mg/dl safety constraint. It is worth mentioning at this stage that the closed-loop performance of the proposed algorithm is safe and effective. It is also important to note that the average time spent in the euglycemic range (70-180 mg/dl) by the three subjects is found to be approximately equal to 77%, 73% and 76%, respectively, for scenarios 2A-2D. It validates the effectiveness of the proposed control algorithm in achieving improved glycemic control.

3.2.5. Quantitative performance evaluation of the closed loop simulations

The two most important features of the analysis of any glucose regulation algorithm are safety and efficacy. The former

is investigated extensively in the previous simulation scenarios. The later is being investigated in the current section. Several important performance indices that are critical to evaluate the closed-loop glucose regulation include the Low Glucose Variability Index (LBGI), High Glucose Variability Index (HBGI), Coefficient of Variation (CoV), mean blood glucose and HbA1c [54]. The LBGI and HBGI for the Scenarios 2A-2D are presented as bar plots, as illustrated in Fig. 6. The rest of the indices are computed, and the corresponding results are summarised in Table 5.

Table 5: Statistical analysis of the closed loop results obtained during Scenario 2A-2D.

Subject	Scenario No.	Mean glucose (mg/dl)	CoV (%)	HbA1c (%)
Subject 1	2A	148.69	0.0222	6.8081
	2B	136.48	0.0229	6.3827
	2C	152.31	0.1325	6.9342
	2D	148.99	0.1195	6.6791
Subject 3	2A	144.98	0.1087	6.6791
	2B	145.56	0.9910	6.6991
	2C	139.96	0.2022	6.5039
	2D	140.69	0.1945	6.5294
Subject 5	2A	114.23	0.1113	5.6076
	2B	111.26	0.0811	5.5040
	2C	112.75	0.1884	5.5559
	2D	110.90	0.1891	5.4916

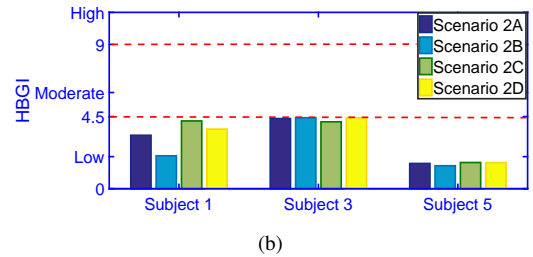
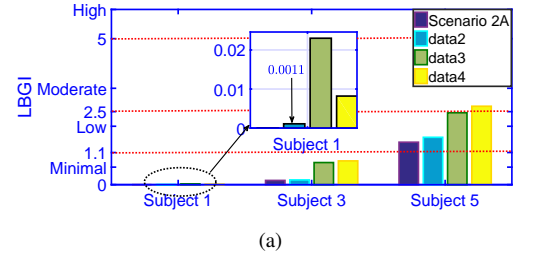


Figure 6: LBGI and HBGI for the (a) subject 1, (b) subject 2 and (c) subject 3 for Scenarios 2A-2D.

The statistical results of the closed-loop simulations of Scenario 2A-2D are thoroughly summarized in Table 5. The mean glucose level of 136.48-152.31 mg/dl, 139.96-145.56 mg/dl, and 110.90-114.23 mg/dl are maintained for all the virtual T1D subjects under large perturbations. The quality of glycemic regulation obtained by the proposed observer-based controller is reflected with around HbA1c of 6.5%, which is one of the

main aims of any standard diabetes treatment [55]. The above-mentioned facts can also be verified from the attainment of a low value of Coefficient of Variability (CoV). In all the cases, CoV is below 2%, which is an indicator of low glucose variability under the feedback action. The LBGi and HBGI predict the risk of hypoglycemia and hyperglycemia, respectively. The risk analysis that is directly related to the reliability of any glucose controller depends on these two factors. The LBGi and HBGI for Subjects 1, 3, and 5 are presented in a bar plot in Fig. 6. It can be easily observed from Fig. 6(a) that the LBGi for Subject 1 and 3 are in the minimal LBGi region ($LBGi < 1.1$), which is significant in avoiding the risks of hypoglycemia. For T1D subject 5, LBGi is low. The corresponding HBGI are also in the Low LBGi region, as illustrated in Fig. 6(b). Hence, the results validate that the risks related to the postprandial hyperglycemia are low under the designed control action.

4. Conclusion

The concept of contraction analysis is utilized in the present work for designing an observer and a controller to achieve a tight glycemic control in the presence of intra-patient variability. The proposed method is shown to be effective in handling intra-patient variability resulting from different sources of uncertainty. Extensive numerical simulations are carried out to evaluate the performance of the proposed technique for realistic scenarios. The postprandial hyperglycemic events are significantly minimized, and hypoglycemia is avoided. The efficacy of the control algorithm is evaluated through statistical analysis. The simple structure of the observer and control law makes it a desirable candidate for Artificial Pancreas. The control scheme can be extended to more complicated models like the UVa Padova model, Hovorka model, etc., that consider a detailed dynamics where the effect of glucagon and free fatty acids. The design philosophy can be extended for nonlinear systems with a quantized and sampled output, which represents the actual glucose measurements done by the CGM devices in practice.

Conflicts of interest

The authors declare no conflicts of interest.

References

- [1] A. Cinar, Artificial pancreas systems: An introduction to the special issue, *IEEE Control Systems Magazine* 38 (1) (2018) 26–29.
- [2] D. Majdpour, M. Tsoukas, J.-F. Yale, A. Haidar, 19 - a fully-automated artificial pancreas to alleviate the burden of carbohydrate counting in type 1 diabetes, *Canadian Journal of Diabetes* 43 (7, Supplement) (2019) S8, 2019 Abstract Issue. doi:<https://doi.org/10.1016/j.jcjd.2019.07.026>.
- [3] P. Bjornstad, K. C. Donaghue, D. M. Maahs, Macrovascular disease and risk factors in youth with type 1 diabetes: time to be more attentive to treatment?, *The Lancet Diabetes & Endocrinology* 6 (10) (2018) 809 – 820. doi:[https://doi.org/10.1016/S2213-8587\(18\)30035-4](https://doi.org/10.1016/S2213-8587(18)30035-4).
- [4] Complications of type 1 diabetes (Jul 2019).

- [5] J. Bondia, S. Romero-Vivo, B. Ricarte, J. L. Diez, Insulin estimation and prediction: A review of the estimation and prediction of subcutaneous insulin pharmacokinetics in closed-loop glucose control, *IEEE Control Systems Magazine* 38 (1) (2018) 47–66.
- [6] Y. Ruan, M. E. Wilinska, H. Thabit, R. Hovorka, Modeling day-to-day variability of glucose–insulin regulation over 12-week home use of closed-loop insulin delivery, *IEEE Transactions on Biomedical Engineering* 64 (6) (2017) 1412–1419.
- [7] L. M. Huyett, E. Dassau, H. C. Zisser, F. J. Doyle, Glucose sensor dynamics and the artificial pancreas: The impact of lag on sensor measurement and controller performance, *IEEE Control Systems Magazine* 38 (1) (2018) 30–46.
- [8] B. W. Bequette, F. Cameron, B. A. Buckingham, D. M. Maahs, J. Lum, Overnight hypoglycemia and hyperglycemia mitigation for individuals with type 1 diabetes: How risks can be reduced, *IEEE Control Systems Magazine* 38 (1) (2018) 125–134.
- [9] G. Marchetti, M. Barolo, L. Jovanović, H. Zisser, D. E. Seborg, A feedforward–feedback glucose control strategy for type 1 diabetes mellitus, *Journal of Process Control* 18 (2) (2008) 149 – 162. doi:<https://doi.org/10.1016/j.jprocont.2007.07.008>.
- [10] Artificial pancreas clinical trials: Moving towards closed-loop control using insulin-on-board constraints, *Biomedical Signal Processing and Control* 45 (2018) 1 – 9. doi:<https://doi.org/10.1016/j.bspc.2018.05.009>.
- [11] A. Nath, R. Dey, Robust guaranteed-cost output feedback control of blood glucose in type 1 diabetes patient with inpatient variability, *Optimal Control Applications and Methods* n/a (n/a). doi:[10.1002/oca.2607](https://doi.org/10.1002/oca.2607).
- [12] A. Nath, D. Deb, R. Dey, Robust observer-based adaptive control of blood glucose in diabetic patients, *International Journal of Control* 0 (0) (2020) 1–14. doi:[10.1080/00207179.2020.1750705](https://doi.org/10.1080/00207179.2020.1750705).
- [13] A. Nath, R. Dey, Robust observer based control for plasma glucose regulation in type 1 diabetes patient using attractive ellipsoid method, *IET Systems Biology* 13 (2) (2019) 84–91.
- [14] A. M. Hariri, Identification, state estimation, and adaptive control of type 1 diabetic patients.
- [15] A. Nath, R. Dey, C. Aguilar-Avelar, Observer based nonlinear control design for glucose regulation in type 1 diabetic patients: An lmi approach, *Biomedical Signal Processing and Control* 47 (2019) 7 – 15. doi:<https://doi.org/10.1016/j.bspc.2018.07.020>.
- [16] P. Biswas, S. Bhaumik, I. Patiyat, Estimation of glucose and insulin concentration using nonlinear gaussian filters, in: 2016 IEEE First International Conference on Control, Measurement and Instrumentation (CMI), 2016, pp. 16–20.
- [17] S. Girardot, F. Mousin, J. Vezinet, P. Jacquemier, S. Hardy, J.-P. Riveline, Kalman filter-based novel methodology to assess insulin pump accuracy, *Diabetes Technology & Therapeutics* 21 (10) (2019) 557–565, PMID: 31335164. doi:[10.1089/dia.2019.0147](https://doi.org/10.1089/dia.2019.0147).
- [18] D. de Pereda, S. Romero-Vivo, B. Ricarte, P. Rossetti, F. J. Ampudia-Blasco, J. Bondia, Real-time estimation of plasma insulin concentration from continuous glucose monitor measurements, *Computer Methods in Biomechanics and Biomedical Engineering* 19 (9) (2016) 934–942, PMID: 26343364. doi:[10.1080/10255842.2015.1077234](https://doi.org/10.1080/10255842.2015.1077234).
- [19] C. Eberle, C. Ament, The unscented kalman filter estimates the plasma insulin from glucose measurement, *Biosystems* 103 (1) (2011) 67–72.
- [20] C. M. Ramkissoon, A. Bertachi, A. Beneyto, J. Bondia, J. Vehi, Detection and control of unannounced exercise in the artificial pancreas without additional physiological signals, *IEEE Journal of Biomedical and Health Informatics* 24 (1) (2020) 259–267.
- [21] B. Singh, S. Kamal, D. Ghosh, S. Ghosh, A. Ferrara, A. K. Pal, J. K. Goyal, Controller and observer design using vector framework with simplified contraction analysis, in: 2020 IEEE International Conference on Industrial Technology (ICIT), 2020, pp. 29–34.
- [22] A. Nath, S. Biradar, A. Balan, R. Dey, R. Padhi, Physiological models and control for type 1 diabetes mellitus: A brief review, *IFAC-PapersOnLine* 51 (1) (2018) 289 – 294, 5th IFAC Conference on Advances in Control and Optimization of Dynamical Systems ACODS 2018. doi:<https://doi.org/10.1016/j.ifacol.2018.05.077>.
- [23] H. Blauw, P. Keith-Hynes, R. Koops, J. H. DeVries, A review of safety and design requirements of the artificial pancreas, *Annals of biomedical engineering* 44 (11) (2016) 3158–3172.
- [24] R. A. Lal, L. Ekhlaspour, K. Hood, B. Buckingham, Realizing

- a Closed-Loop (Artificial Pancreas) System for the Treatment of Type 1 Diabetes, *Endocrine Reviews* 40 (6) (2019) 1521–1546. doi:10.1210/er.2018-00174.
- [25] E. Ruiz-Velázquez, R. Femat, D. U. Campos-Delgado, Blood glucose control for type i diabetes mellitus: A robust tracking hoo problem, 2004.
- [26] S. Mandal, A. Bhattacharjee, A. Sutradhar, Lmi based robust blood glucose regulation in type-1 diabetes patient with daily multi-meal ingestion, *Journal of The Institution of Engineers (India): Series B* 95 (2) (2014) 121–128.
- [27] P. Colmegna, R. S. Sánchez Peña, R. Gondhalekar, E. Dassau, F. J. Doyle III, Reducing risks in type 1 diabetes using ∞ control, *IEEE Transactions on Biomedical Engineering* 61 (12) (2014) 2939–2947.
- [28] S. Ahmad, NasimUllah, N. Ahmed, M. Ilyas, W. Khan, Super twisting sliding mode control algorithm for developing artificial pancreas in type 1 diabetes patients, *Biomedical Signal Processing and Control* 38 (2017) 200–211. doi:https://doi.org/10.1016/j.bspc.2017.06.009.
- [29] A. G. Gallardo Hernández, L. Fridman, A. Levant, Y. Shtessel, R. Leder, C. Revilla Monsalve, S. Islas Andrade, High-order sliding-mode control for blood glucose: Practical relative degree approach, *Control Engineering Practice* 21 (5) (2013) 747 – 758. doi:https://doi.org/10.1016/j.conengprac.2012.11.015.
- [30] X. Yu, O. Kaynak, Sliding mode control made smarter: A computational intelligence perspective, *IEEE Systems, Man, and Cybernetics Magazine* 3 (2) (2017) 31–34.
- [31] A. Revert, F. Garelli, J. Picó, H. De Battista, P. Rossetti, J. Vehi, J. Bondia, Safety auxiliary feedback element for the artificial pancreas in type 1 diabetes, *IEEE Transactions on Biomedical Engineering* 60 (8) (2013) 2113–2122.
- [32] C. M. Ramkissoon, B. Aufderheide, B. W. Bequette, J. Vehí, A review of safety and hazards associated with the artificial pancreas, *IEEE Reviews in Biomedical Engineering* 10 (2017) 44–62.
- [33] S. Samadi, K. Turksoy, I. Hajizadeh, J. Feng, M. Sevil, A. Cinar, Meal detection and carbohydrate estimation using continuous glucose sensor data, *IEEE Journal of Biomedical and Health Informatics* 21 (3) (2017) 619–627.
- [34] K. Turksoy, E. Littlejohn, A. Cinar, Multimodule, multivariable artificial pancreas for patients with type 1 diabetes: Regulating glucose concentration under challenging conditions, *IEEE Control Systems Magazine* 38 (1) (2018) 105–124.
- [35] J. Jouffroy, Some ancestors of contraction analysis, in: *Proceedings of the 44th IEEE Conference on Decision and Control*, 2005, pp. 5450–5455.
- [36] W. Lohmiller, J.-J. E. Slotine, On contraction analysis for non-linear systems, *Automatica* 34 (6) (1998) 683 – 696. doi:https://doi.org/10.1016/S0005-1098(98)00019-3.
- [37] B. B. Sharma, I. N. Kar, Design of asymptotically convergent frequency estimator using contraction theory, *IEEE Transactions on Automatic Control* 53 (8) (2008) 1932–1937.
- [38] M. M. Rayguru, I. N. Kar, High gain observer-based saturated controller for feedback linearizable system, *IEEE Transactions on Circuits and Systems II: Express Briefs* 67 (1) (2019) 122–126.
- [39] E. M. Aylward, P. A. Parrilo, J.-J. E. Slotine, Stability and robustness analysis of nonlinear systems via contraction metrics and sos programming, *Automatica* 44 (8) (2008) 2163 – 2170. doi:https://doi.org/10.1016/j.automatica.2007.12.012.
- [40] S. S. Kanderian, S. Weinzimer, G. Voskanyan, G. M. Steil, Identification of intraday metabolic profiles during closed-loop glucose control in individuals with type 1 diabetes, *Journal of Diabetes Science and Technology* 3 (5) (2009) 1047–1057, pMID: 20144418. doi:10.1177/193229680900300508.
- [41] K. Turksoy, I. Hajizadeh, S. Samadi, J. Feng, M. Sevil, M. Park, L. Quinn, E. Littlejohn, A. Cinar, Real-time insulin bolusing for unannounced meals with artificial pancreas, *Control Engineering Practice* 59 (2017) 159 – 164. doi:https://doi.org/10.1016/j.conengprac.2016.08.001.
- [42] I. Sala-Mira, J.-L. Diez, B. Ricarte, J. Bondia, Sliding-mode disturbance observers for an artificial pancreas without meal announcement, *Journal of Process Control* 78 (2019) 68 – 77. doi:https://doi.org/10.1016/j.jprocont.2019.03.008.
- [43] P. Liò, P. Zuliani, *Automated Reasoning for Systems Biology and Medicine*, Vol. 30, Springer, 2019.
- [44] N. Resalat, J. E. Youssef, R. Reddy, P. G. Jacobs, Evaluation of model complexity in model predictive control within an exercise-enabled artificial pancreas, *IFAC-PapersOnLine* 50 (1) (2017) 7756 – 7761, 20th IFAC World Congress. doi:https://doi.org/10.1016/j.ifacol.2017.08.2270.
- [45] A. Nath, D. Deb, R. Dey, An augmented subcutaneous type 1 diabetic patient modelling and design of adaptive glucose control, *Journal of Process Control* 86 (2020) 94 – 105. doi:https://doi.org/10.1016/j.jprocont.2019.08.010.
- [46] J. Garcia-Tirado, C. Zuluaga-Bedoya, M. D. Breton, Identifiability analysis of three control-oriented models for use in artificial pancreas systems, *Journal of Diabetes Science and Technology* 12 (5) (2018) 937–952, pMID: 30095007. doi:10.1177/1932296818788873.
- [47] R. Sanz, P. Garcia, J. Diez, J. Bondia, Artificial pancreas system with unannounced meals based on a disturbance observer and feedforward compensation, *IEEE Transactions on Control Systems Technology* (2020) 1–7.
- [48] D. R. L. Worthington, Minimal model of food absorption in the gut, *Medical Informatics* 22 (1) (1997) 35–45. doi:10.3109/14639239709089833.
- [49] W. Lohmiller, J.-J. E. Slotine, On contraction analysis for non-linear systems, *Automatica* 34 (6) (1998) 683–696.
- [50] M. Vidyasagar, On matrix measures and convex liapunov functions, *Journal of Mathematical Analysis and Applications* 62 (1) (1978) 90–103.
- [51] Z. Aminzare, E. D. Sontagy, Contraction methods for nonlinear systems: A brief introduction and some open problems, in: *53rd IEEE Conference on Decision and Control*, IEEE, 2014, pp. 3835–3847.
- [52] J. Jouffroy, T. I. Fossen, A tutorial on incremental stability analysis using contraction theory.
- [53] W. Wang, J.-J. E. Slotine, On partial contraction analysis for coupled nonlinear oscillators, *Biological cybernetics* 92 (1) (2005) 38–53.
- [54] B. P. Kovatchev, W. L. Clarke, M. Breton, K. Brayman, A. McCall, Quantifying temporal glucose variability in diabetes via continuous glucose monitoring: mathematical methods and clinical application, *Diabetes technology & therapeutics* 7 (6) (2005) 849–862.
- [55] O. Schnell, J. B. Crocker, J. Weng, Impact of hba1c testing at point of care on diabetes management, *Journal of Diabetes Science and Technology* 11 (3) (2017) 611–617.